SEISMIC PERFORMANCE FACTORS FOR STEEL ECCENTRICALLY BRACED FRAMES

Cem Topkaya
Professor of Civil Engineering
Middle East Technical University
Ankara, Turkey
e-mail: ctopkaya@metu.edu.tr

Ahmet Kuşyılmaz
Graduate Student
Middle East Technical University
Ankara, Turkey
e-mail: e133798@metu.edu.tr

ABSTRACT

This paper describes a numerical study undertaken to evaluate the seismic performance factors for steel eccentrically braced frames (EBFs). The response modification (*R*), overstrength (Ω_o), and deflection amplification (C_d) factors recommended in ASCE7-10 for EBFs were evaluated by making use of the methodology outlined in FEMA P695. Nonlinear time history analyses were conducted on 12 archetype EBFs. The results indicate that EBFs accumulate damage at the bottom stories. For structures located in Seismic Design Category D_{max} the average of the link rotation angles under the Maximum Considered Earthquake were found to exceed 0.2 radians which can lead to link fractures. On the other hand, the bottom story links of structures located in Seismic Design Category D_{min} were found to experience much lower rotation angle demands. In light of these findings, modifications to the displacement amplification factors were proposed and structures located in Seismic Design Category D_{max} were re-designed according to the these modifications. The performances of re-designed frames were evaluated using the same methodology. The results indicate that the proposed modifications reduce the rotation angle demands such that the maximums vary between 0.11 and 0.16 radians.

INTRODUCTION

Eccentrically braced frames (EBFs) are among various lateral load resisting systems for steel structures under seismic loading [1]. A typical EBF is composed of links, beams, columns and braces as shown in Fig. 1. The braces are connected to the beams with an eccentricity and create a short segment between connection points called the link beam. Very high shear forces and bending moments are produced on the links under the action of lateral loads which are produced by seismic actions. High amounts of shear force and bending moment cause yielding of the link which eventually contributes to energy dissipation. Type of yielding is usually related with the length and size of the link. Normalized link length ($e/(M_p/V_p)$), where e is the link length, M_p is the plastic moment capacity of the link, and V_p is the plastic shear capacity of the link, is used to describe the yielding mechanism. Short links ($e/(M_p/V_p) \leq 1.6$), yield primarily under shear while long links ($e/(M_p/V_p) \geq 2.6$) yield primarily under flexure. Intermediate links ($1.6 < e/(M_p/V_p) < 2.6$) yield under both shear and flexure.

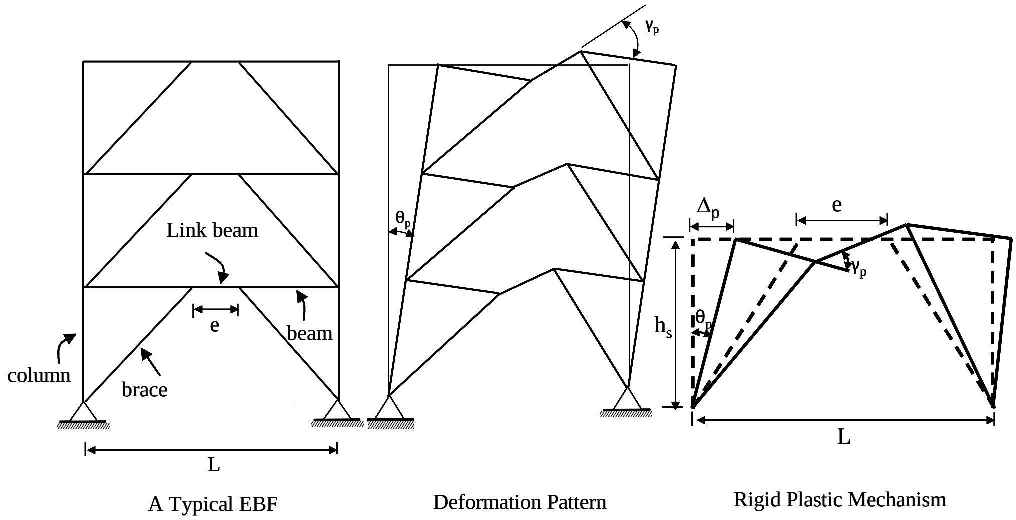

Fig. 1 A typical EBF and deformation pattern

Links are the primary source of energy dissipation in EBFs. As shown in Fig. 1, links yield and deform under lateral loading while the beams outside of the link, the braces and the columns are expected to remain elastic. The inelastic deformation capacity of the links depends on the normalized link length and stiffening of the link. In general, link rotation angle (γ_p), shown in Fig. 1, is used a measure of inelastic deformation. By definition, the link rotation angle is the plastic rotation angle between the link and the beam outside of the link. The link rotation angle limits usually vary between 0.02 radians and 0.08 radians.

The most accurate way of estimating link rotation angle demands is to conduct a nonlinear time history analysis. This type of analysis is onerous and is not generally used in routine design practice. Alternatively, the link rotation angle demands can be estimated using the rigid-plastic mechanism offered by the Commentary to the AISC Seismic Provisions for Structural Steel Buildings (AISC341) [2]. The link rotation angle is expressed in terms of the plastic story drift (Δ_p) by making use of geometrical relationships. For the commonest EBF configuration where the link is a horizontal framing member located in between braces (Fig. 1) the link rotation angle can be expressed as follows:

$$\gamma_p = \frac{L}{e}\frac{\Delta_p}{h_s} \tag{1}$$

where L is the bay width, and h_s is the height of the story.

The Commentary to the AISC Seismic Provisions for Structural Steel Buildings (AISC341) [2] recommends that the plastic story drift can be conservatively taken as the design story drift. The equivalent lateral force procedure can be used together with a set of seismic response factors to obtain the design story drift. This procedure enables elastic analysis and design which is based on reduced seismic forces. The idea here is that the amount of lateral forces is reduced by taking into account yielding and ductility of the lateral load resisting system. The general structural response shown in Fig. 2 can be considered to develop response factors. Their formulation according to Uang [3] is as follows:

$$\mu_s = \frac{\Delta_{\max}}{\Delta_y} \quad R_\mu = \frac{V_e}{V_y} \quad \Omega_o = \frac{V_y}{V_s} \quad R = \frac{V_e}{V_s} = R_\mu \Omega_o \quad C_d = \frac{\Delta_{\max}}{\Delta_s} = \mu_s \Omega_o \tag{2}$$

where, V_e is the ultimate elastic base shear, V_s is the base shear at the first significant yield, V_y is the base shear at the structural collapse level, Δ_s is the drift at the first significant yield, Δ_y is the drift at the structural collapse level, Δ_{max} is the maximum amount of drift, μ_s is the ductility factor, Ω_o is the overstrength factor, R_μ is the ductility reduction factor, R is the response modification factor, and C_d is the deflection amplification factor.

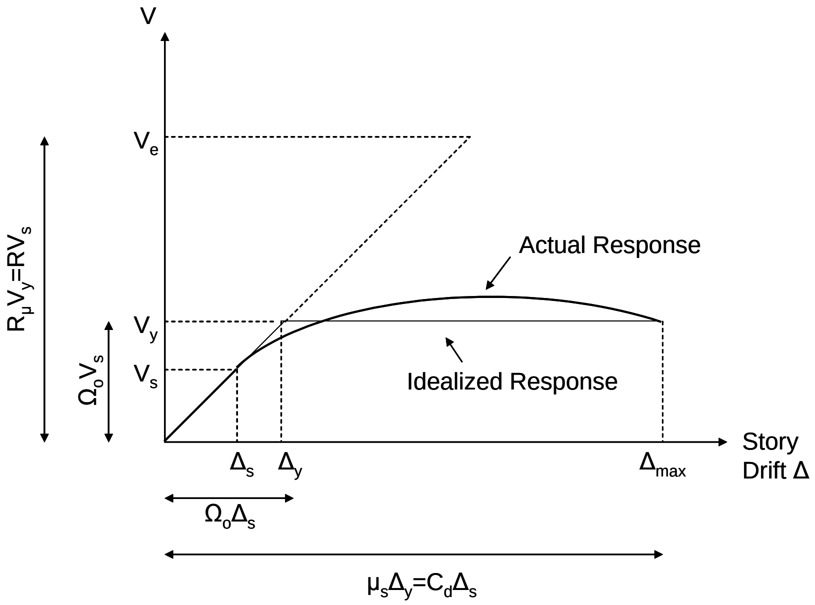

Fig. 2 General structural response

Lateral forces due to seismic action are reduced by a response modification factor (R) and the structure is designed using these reduced forces. The displacements from the elastic analysis employing equivalent lateral force procedure are less than the displacements of the structure which yields during a seismic event. In order to predict these displacements, the displacements from elastic analysis must be amplified by a deflection amplification factor (C_d). The amplified displacements are subsequently used in design.

Seismic response factors were developed for various lateral load resisting systems based on observations from past earthquakes and engineering judgment. These factors vary from one specification to the other. In the United States, seismic response factors for EBFs are given in Minimum Design Loads for Buildings and Other Structures [4] hereafter referred as ASCE7-10. The recommended values of the response modification factor (R), the overstrength factor (Ω_o), and the deflection amplification factor (C_d) are 8, 2, and 4, respectively. In Europe, the seismic response factors for EBFs are given in Eurocode 8 [5]. The recommended value of the response modification factor (R) and deflection amplification factor (C_d) is 6 unless a more detailed nonlinear static pushover analysis is conducted. Eurocode 8 has a more different approach than the seismic codes in the United States and does not recommend a single value for the overstrength factor (Ω_o).

Satisfactory performance has been observed for EBFs subjected to earthquakes until 2010. Buildings employing EBFs as a lateral load resisting system were investigated after the 2010 and 2011 New Zealand earthquakes. These investigations revealed that some of the link beams fractured [6] and showed an undesired performance. A research project has been initiated at Middle East Technical University in light of the observation from New Zealand earthquakes. The aim of the project is to study seismic response factors for EBFs and provide design recommendations. Each of the response factors were studied in detail through nonlinear time history analysis. The final phase of the project involves application of FEMA P695 Methodology [7] to EBFs to determine the adequacy of seismic response factors that are recommended in ASCE7-10. This paper presents the preliminary studies conducted as a part of the final phase of this research project.

OVERVIEW OF THE FEMA P695 METHODOLOGY

A methodology has been developed as a part of the ATC-63 Project and published under the FEMA P695 document [7] entitled "Quantification of Building Seismic Performance Factors". The Methodology can be used to define seismic performance factors for emerging lateral load resisting systems as well as to evaluate these factors for existing systems. The idea behind the Methodology is to produce performance groups which consist of archetype designs. By definition, the archetypes capture the essence and variability of performance characteristics of the system of interest. The idea is not to find out the most problematic cases but to represent the general behavior possessed by most typical designs that characterize a system. The performance groups are formed by considering the most influential variables such as building height, fundamental period, framing configuration, bay sizes, gravity loads, and etc. These groups reflect major divisions, or changes in behavior, within the archetype design space.

The Methodology requires nonlinear collapse simulation on the selected archetype models. Collapse simulation is conducted using a far field record set that consists of 22 pairs of ground motions. All 44 ground motions records must be individually applied to an archetype in cases where a two dimensional analysis is performed. The ground motion records are scaled twice. The first scaling is required to anchor the median spectrum of the far field record set to the Maximum Considered Earthquake (MCE) response spectra at the fundamental period of the archetype. The second scaling is applied successively to all far field ground motions until 50 percent of the archetypes exhibit collapse. The amount of scaling that results in the collapse of 50 percent of the archetypes is compared with a variable named the Adjusted Collapse Margin Ratio (*ACMR*). The target *ACMR* values are tabulated in the FEMA P695 document and depend on the total system collapse uncertainty (β_{TOT}), and collapse probability. Two conditions must be satisfied for acceptable performance. The average value of *ACMR* for each performance group should meet the target *ACMR* for 10 percent collapse probability ($ACMR_{10\%}$). Furthermore, individual values of *ACMR* for each index archetype within a performance group should meet the target *ACMR* for 20 percent collapse probability ($ACMR_{20\%}$).

The total system collapse uncertainty (β_{TOT}) depends on various factors such as record-to-record collapse uncertainty, design requirements-related collapse uncertainty, test data-related collapse uncertainty, and modeling-related collapse uncertainty. The methodology enables to use non-simulated collapse models for collapse failure modes that cannot be explicitly modeled. Non-simulated collapse modes can be indirectly evaluated using alternative limit state checks on structural response quantities measured in the analysis. Fracture in the connections and hinge regions of steel moment frame components are examples of possible non-simulated collapse modes.

DESIGN AND SELECTION OF ARCHETYPES

The study presented herein was conducted to gain an insight into the performance of EBF archetypes. Some of the steps of the Methodology were deliberately modified because the present study is a preliminary investigation. The idea here is to study various archetypes and distinguish important variables that result in systems where the performance does not reach to acceptable levels. The first modification was on scaling of the record set. The Methodology requires scaling the records beyond the MCE level to arrive at collapse probabilities. In the present study it was decided to evaluate the performance of archetypes at the Maximum Considered Earthquake (MCE) level. If the performance objectives cannot be met at the MCE level ground motions it implies that the performance levels cannot be met at higher demands obtained using scaling of the records.

EBF systems exhibit high ductility and energy dissipation capacity. Because of its superior performance over other lateral load resisting systems EBFs are usually preferred in high and very high seismic regions. Different Seismic Design Categories (SDC) can be adopted in the Methodology in order to represent the variation in seismic hazard. In the present study two seismic design categories namely SDC D_{max} and SDC D_{min} were considered. The MCE, 5 percent damped, spectral response acceleration parameter at short periods adjusted after site class effects (S_{MS}) is taken 1.50g and 0.75g for SDC D_{max}, and SDC D_{min}, respectively. The MCE, 5 percent damped, spectral response acceleration parameter at a period of 1 sec adjusted after site class effects (S_{M1}) is taken 0.90g and 0.30g for SDC D_{max}, and SDC D_{min}, respectively.

Two geometric configurations are typically used for EBFs. In the first and commonest configuration shown in Fig. 1, the link beam is a horizontal member located in between the braces. Alternatively one end of the brace can be connected to the column. This second configuration was found to be problematic because of the link to column connection details [8]. The 2010 version of the Commentary to the AISC Seismic Provisions for Structural Steel Buildings [9] recommends avoiding EBF configurations with links attached to columns until further research on link to column connections is available. Because of this reason only one EBF configuration shown in Fig. 1 was considered in this study.

Only one type of floor plan shown in Fig. 3 was considered. The floor plan is square with side dimensions of 30 meters. There are three bays in each bent and the center bay consists of an EBF. The beam to column connections of the EBF bay was considered rigid and all other beam to columns connections were considered simple. A dead load of 5 kN/m^2 and a live load of 2 kN/m^2 which are typical for steel office buildings were considered as loading. Story height was taken as 3.5 meters for all stories. In order to take into account variations in structural periods, 3, 6 , and 9 story EBFs were considered. EBF bay width was also considered as a variable. Bay widths of 6 meters and 10 meters were considered. While the bay width of EBFs changes it was assumed that the side dimensions of the floor plan remains constant.

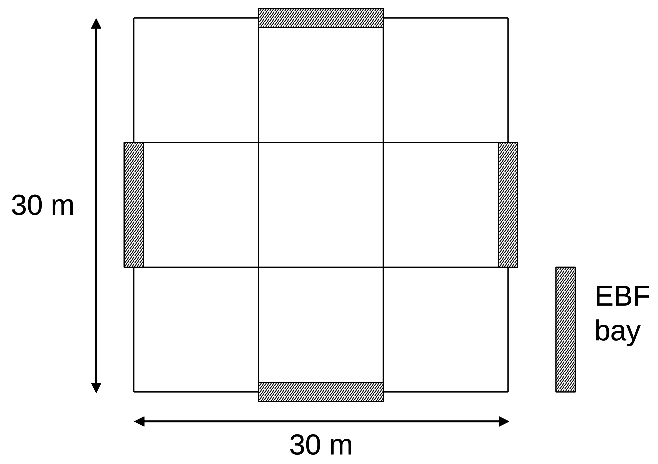

Fig. 3 Floor plan used for the study

As discussed before the normalized link length is an important parameter that influences the behavior of links. Most of the links used in practice are short links that primarily yield in shear [10]. In the present study only the behavior of short links was considered. Therefore, the link sections were selected to satisfy $e/(M_p/V_p) \leq 1.6$. The link length to bay width ratio (e/L) was considered as 0.1 for all archetypes.

Variations in Seismic Design Category, number of stories, and EBF bay width resulted in 12 archetypes to be considered in the parametric study. A992 grade steel with a yield strength of 345 MPa was considered for all framing members. Designs were conducted according to ASCE 7-10 [4], AISC 341-05 [2], and AISC 360-05 [11]. Archetypes were designed by minimizing the weight of the framing. Details of the design process are explained in Kuşyılmaz and Topkaya [12]. Link, brace, and column members of 12 archetypes are given in Table 1. Selection of link sections are governed by either strength or stiffness requirements. For most of the frames designed according to SDC D_{max} link rotation angle provisions governed the sizing of link sections. Only for 3 story frames strength was the governing criterion. The link rotation angle limit of 0.08 radians imposed on shear yielding links provides a stringent stiffness criterion. Link sizes have to be increased in most cases to meet this limit. Selection of link sections for frames designed according to SDC D_{min} was influenced by other criteria. Firstly, the link sections had to be selected from a pool of rolled shapes which satisfy shear yielding link criterion ($e/(M_p/V_p) \leq 1.6$). This constraint reduced the number of rolled shapes available. Secondly, the stability of the beam outside of the link imposes further constraints on the design. In general this member is under high axial force and bending moments. In the present study the link and the beam were assumed to have the same member size. Therefore, the link sections that satisfy the stability provisions for the beam outside of the link were used in the selection process and this further reduced the pool of available sections. As indicated in Table 1 these constraints resulted in over-designed link members and in some cases using the same link member in all stories. The following section outlines the numerical analysis of these archetypes.

Story	Link	Brace	Column	Link	Brace	Column
	SDC D_{max} L=6m ns=3			SDC D_{min} L=6m ns=3		
1	W16×31	W8×40	W14×68	W6×25	W8×28	W14×48
2	W16×31	W8×40	W14×68	W5×19	W6×25	W14×48
3	W10×19	W14×38	W14×68	W5×16	W6×25	W14×48
	SDC D_{max} L=6m ns=6			SDC D_{min} L=6m ns=6		
1	W18×46	W8×58	W14×132	W6×25	W8×28	W14×68
2	W18×46	W8×58	W14×132	W6×25	W8×28	W14×68
3	W18×46	W8×58	W14×132	W6×25	W8×28	W14×68
4	W18×46	W8×58	W14×74	W5×19	W6×25	W14×48
5	W18×40	W8×48	W14×74	W5×16	W6×25	W14×48
6	W18×35	W8×48	W14×74	W5×16	W6×25	W14×48
	SDC D_{max} L=6m ns=9			SDC D_{min} L=6m ns=9		
1	W24×62	W14×74	W14×311	W10×19	W14×38	W14×132
2	W24×62	W14×74	W14×311	W10×19	W14×38	W14×132
3	W24×62	W14×74	W14×311	W10×19	W14×38	W14×132
4	W24×62	W14×74	W14×211	W10×19	W14×38	W14×74
5	W24×62	W14×74	W14×211	W8×21	W12×35	W14×74
6	W24×62	W14×74	W14×211	W6×25	W8×28	W14×74
7	W24×62	W14×74	W14×132	W6×25	W8×28	W14×48
8	W24×55	W10×68	W14×132	W6×25	W8×28	W14×48
9	W24×55	W10×68	W14×132	W5×16	W6×25	W14×48
	SDC D_{max} L=10m ns=3			SDC D_{min} L=10m ns=3		
1	W8×40	W8×58	W14×53	W8×40	W8×58	W14×53
2	W8×40	W8×58	W14×53	W8×40	W8×58	W14×53
3	W8×40	W8×58	W14×53	W8×40	W8×58	W14×53
	SDC D_{max} L=10m ns=6			SDC D_{min} L=10m ns=6		
1	W12×35	W14×68	W14×132	W8×40	W8×58	W14×132
2	W12×35	W14×68	W14×132	W8×40	W8×58	W14×132
3	W12×35	W14×68	W14×132	W8×40	W8×58	W14×132
4	W8×40	W8×58	W14×53	W8×40	W8×58	W14×53
5	W8×40	W8×58	W14×53	W8×40	W8×58	W14×53
6	W8×40	W8×58	W14×53	W8×40	W8×58	W14×53
	SDC D_{max} L=10m ns=9			SDC D_{min} L=10m ns=9		
1	W14×38	W14×68	W14×159	W8×40	W8×58	W14×132
2	W14×38	W14×68	W14×159	W8×40	W8×58	W14×132
3	W14×38	W14×68	W14×159	W8×40	W8×58	W14×132
4	W14×38	W14×68	W14×132	W8×40	W8×58	W14×132
5	W14×38	W14×68	W14×132	W8×40	W8×58	W14×132
6	W14×38	W14×68	W14×132	W8×40	W8×58	W14×132
7	W14×38	W14×68	W14×68	W8×40	W8×58	W14×53
8	W12×35	W14×68	W14×68	W8×40	W8×58	W14×53
9	W12×35	W14×68	W14×68	W8×40	W8×58	W14×53

Table 1 Member sizes of archetypes

EVALUATION OF EBF PERFORMANCE

Performances of the designed archetypes were evaluated by making use of numerical analysis. A computational framework named FedeasLab developed by Filippou [13] was used for numerical analysis. This tool is capable of performing nonlinear time history analysis. A novel finite element developed by Saritas and Filippou [14] used for modeling behavior of shear yielding metallic elements is readily available in FedeasLab libraries. This finite element was used to model link beams and all other members were modeled by nonlinear beam elements. Verification of the shear yielding element was conducted by Saritas and Filippou [14] by comparing numerical simulation results with results from individual link experiments. Verification of the numerical models was also conducted at the structure level by Kuşyılmaz [15].

Two-dimensional finite element models were used to model the archetypes. In general, one of the EBF bays was modeled and the tributary mass was added to two of the nodes at every story. A leaner column was also modeled in order to account for the second order effects. The tributary weight of the story was imposed on this leaner column at every story. The archetypes were subjected to 44 ground motion records and the records were scaled to the Maximum Considered Earthquake (MCE) level. A two percent mass and stiffness proportional damping was used in time history analysis.

Evaluation of archetype performance was based on non-simulated collapse models. Link beams generally exhibit stable behavior followed by fracture. As mentioned before fracture in steel members is difficult to simulate and the Methodology allows for non-simulated collapse models where fracture in members is expected. Furthermore, EBFs have little redundancy and when one link fractures the force demand on the fractured link has to be transferred to all the other links which eventually results in overloading and fracture in those links too. In addition, fracture of a link in any one story triggers soft story mechanism which can potentially trigger collapse of the system.

The single most important parameter for evaluating EBF performance is the link rotation angle. All the inelastic action is concentrated in the link beam and the deformation capacity of this member, measured by the link rotation angle, determines how well the system performs under a severe seismic event. The link rotation angles were collected during time history analysis for links in all stories. The maximums of these link rotations were extracted from the time history data. The results for the maximum link rotation angles are given in Figs 4 through 9. In these figures the variation of link rotation angle along the height of the building is given for all 44 ground motions. The median value from the 44 ground motion records is indicated by a solid curve. In addition, the design link rotation angles are shown by filled markers.

The results indicate that there is a significant difference between the behaviors of archetypes designed under different seismic hazards. In general, large differences exist between the design rotation angle and the calculated median link rotation angle. For structures that belong to SDC D_{max} the link rotation angles are observed to exceed the allowable limit of 0.08 radians. For structures designed in SDC D_{min} the median link rotation angles are observed to be less than the allowable value except two cases. This is due to the fact that these systems were over-designed to meet requirements for the beam outside of the link as well as to meet the constraint for shear yielding links.

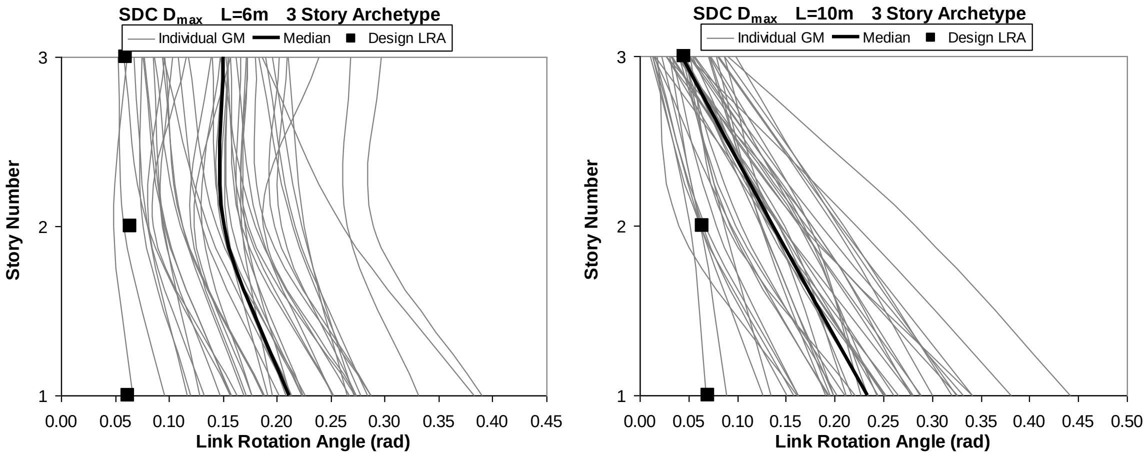

Fig. 4 Variation of link rotation angle for 3 story EBFs (SDC D_{max})

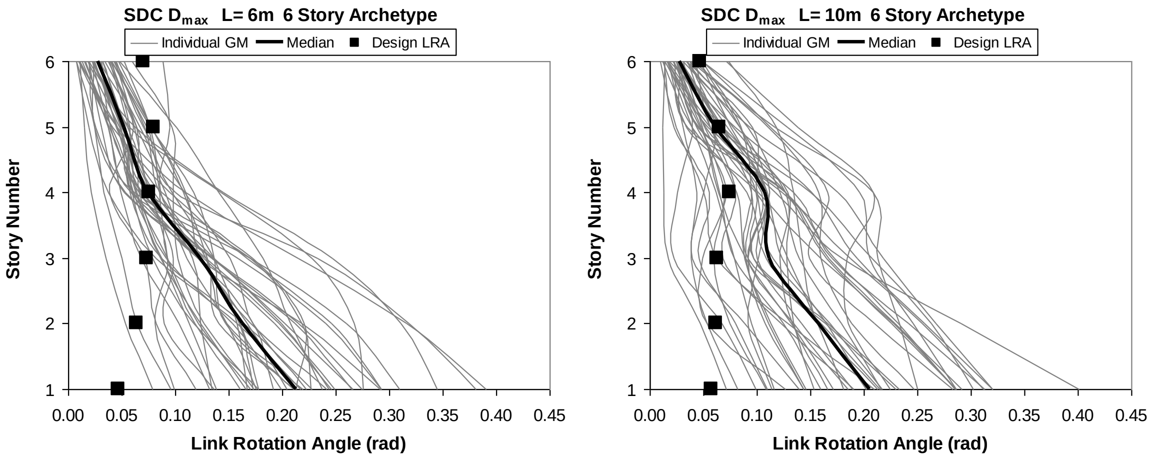

Fig. 5 Variation of link rotation angle for 6 story EBFs (SDC D_{max})

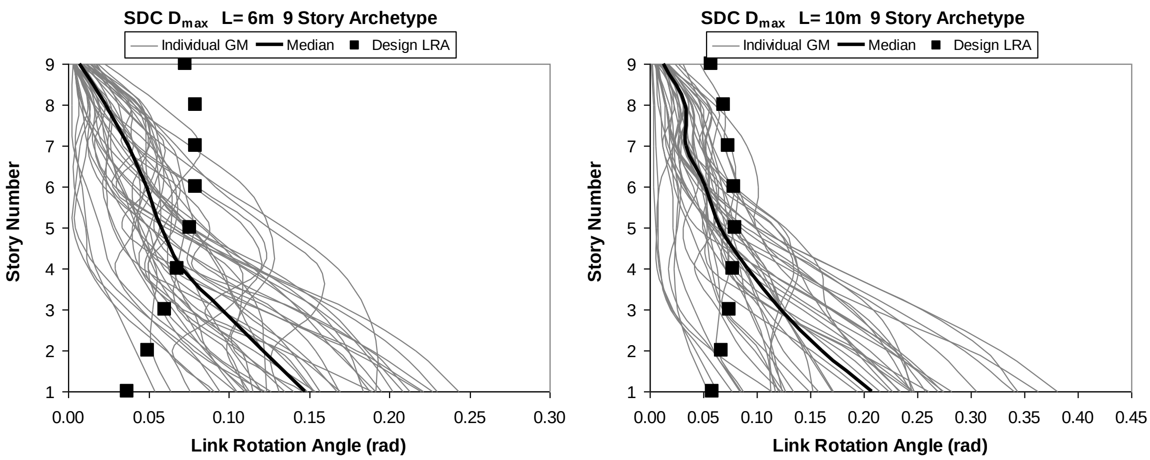

Fig. 6 Variation of link rotation angle for 9 story EBFs (SDC D_{max})

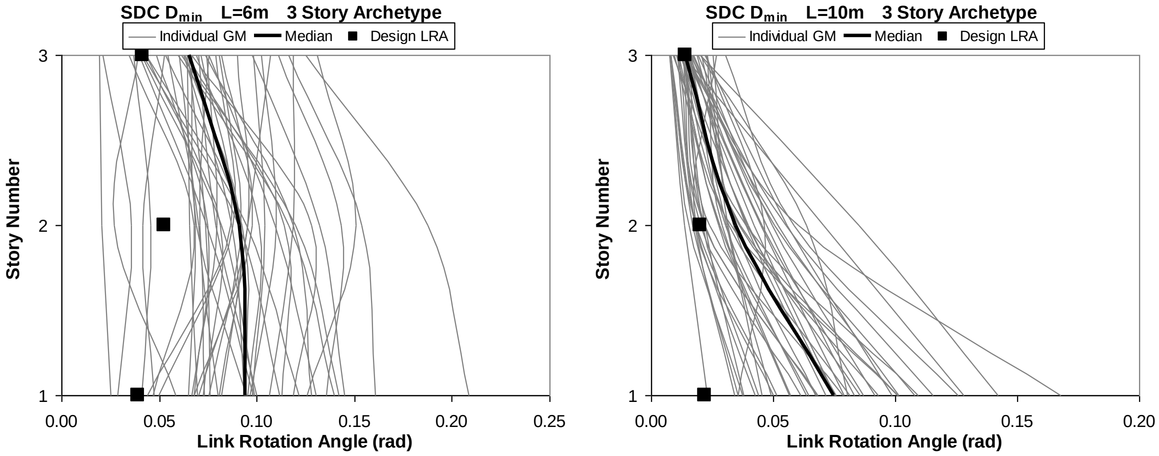

Fig. 7 Variation of link rotation angle for 3 story EBFs (SDC D_{min})

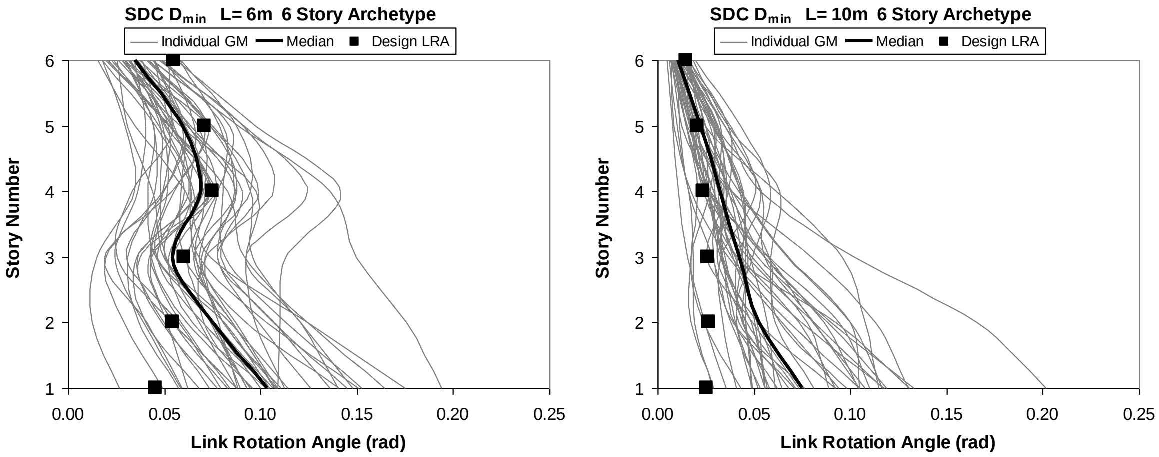

Fig. 8 Variation of link rotation angle for 6 story EBFs (SDC D_{min})

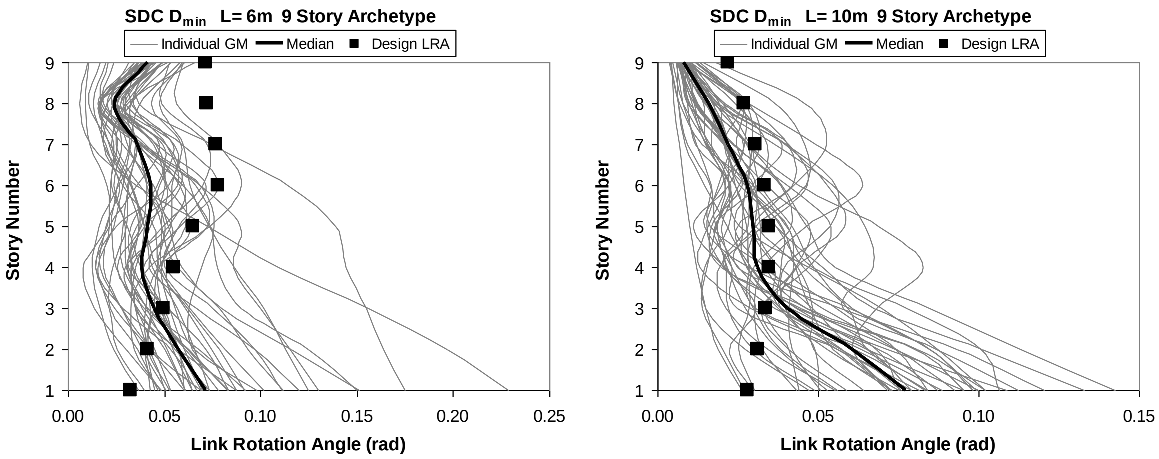

Fig. 9 Variation of link rotation angle for 9 story EBFs (SDC D_{min})

For archetypes designed for SDC D_{max} and having a bay width of 6 meters, the median of the link rotation angles is calculated as 0.21 radians, 0.21 radians, and 0.15 radians for 3, 6, and 9 story structures, respectively. The calculated values for systems with a bay width of 10 meters are equal to 0.23 radians, 0.21 radians, and 0.21 radians for 3, 6, and 9 story structures, respectively. For archetypes designed for SDC D_{min} the median link rotation angles vary between 0.07 radians and 0.10 radians for the bottom story links.

Experiments conducted in the past [16] have shown that links can sustain 0.20 radians of rotation if loaded monotonically. Under cyclic loading however, the link rotation capacity reduces significantly. Under a seismic event a typical link experiences a few cycles with large rotation and a large number of cycles with small rotation demands. Most of the link experiments were conducted using symmetrical cyclic loading cycles and the performance of links under this type of loading is well defined. At a minimum a shear link is expected to sustain 0.08 radians of rotation. Recent experiments conducted by Okazaki et al. [17] showed the complexity of the behavior. Rotation capacity of the links was found to depend on the loading protocol. Links tested under the protocol recommended by the 2002 version of the AISC Seismic Provisions were found to fail before reaching to the 0.08 radian limit. However, links tested under the protocol recommended by the 2005 version of the AISC Seismic Provisions were capable of sustaining rotations in excess of 0.08 radians. In no cases, except monotonic loading, the links were capable of sustaining rotations on the order of 0.20 radians. The numerical analysis results indicate that some corrective measure might be needed to keep the rotation demands at acceptable levels. The recommended values of seismic response factors produce link rotation demands that can result in link fractures. The following section outlines proposed modifications to the seismic response factors.

PROPOSED MODIFICATIONS TO SEISMIC RESPONSE FACTORS

The use of current response factors result in excessive link rotation angle demands at the lower stories. Modifications to the response factors are needed to reduce the maximum level of demand. The work presented herein is part of a larger research study that focuses on the seismic response factors for EBFs. As part of this study each response factor was evaluated in detail. Time history analyses were conducted on typical EBFs by Kuşyılmaz [15] to evaluate the deflection amplification factor. Three, 6, 9, and 12 story EBFs with different e/L ratios, bay width, and seismic hazard were considered. Deflections from nonlinear time history analysis were normalized by the design displacements to arrive at the deflection amplification factor. Typical results for EBFs with different stories are given in Fig. 10. As shown in this figure the value of the C_d factor significantly differs from the codified value of 4 at the lower stories. Underestimation of the displacements at lower stories is the prime reason for having link rotation angle demands that are well beyond the design link rotations.

A variable C_d profile along the height was evaluated as a part of this study to investigate the level of demands for EBFs designed using this profile. It should be noted that the most ideal solution would be to choose a single valued deflection amplification factor. Design specifications do not favor variable response factors along the height of the structure. Choosing C_d a value based on the lower stories however result in significant increases in the overall weight of the framing. In such a case satisfying link rotation angles at the upper stories would be challenging and result in an increase of member sizes in all stories to reduce the deflections. While a single valued deflection amplification factor is preferred, supplementary documents such as the Commentary to the AISC Seismic Provisions [2] can be tailored to provide modifications to the C_d factor. The proposed deflection amplification factor can be expressed as follows:

$$C_{di} = 10 - \frac{6}{7}\left(i - 1\right) \geq 4 \tag{3}$$

where i is the story number, and C_{di} is the deflection amplification factor to be used for the i^{th} story. The variation of the proposed C_d factor is given in Fig. 10 using solid lines. The proposed C_d factor can be used to find out the total story drift which consists of the elastic and plastic components. As given in Eqn 1, the link rotation angle is calculated using the plastic component of story drift. The elastic part should be subtracted from the total to find out the plastic component. In the present study, this was accomplished by modifying the C_d factor. The recommended overstrength value for EBFs is 2.0 and this value is subtracted from the proposed C_d factor in determining the plastic story drift. In other words, the modified version of C_d which is shown in Fig. 10 was directly used to find out the plastic story drifts.

Based on the proposed C_d factor and associated modifications the archetypes were redesigned. Only the EBFs that are designed according to SDC D_{max} were considered because these were the problematic ones. Member sizes of these 6 redesigned archetypes are given in Table 2. The redesigned frames were analyzed using the same set of ground motions. The results for the variation of link rotation angles are given Figs 11, 12, and 13 for 3, 6, and 9 story archetypes, respectively. The maximum of the link rotation angles are observed at the bottommost story and the values vary between 0.11 and 0.12 radians except for one case. For the 3 story archetype with a bay width of 6 meters the maximum value reaches to 0.16 radians.

The results indicate that the use of proposed C_d factor results in a decrease in the link rotation angle demands. Links experimented by Okazaki et al. [17] using the revised loading protocol sustained on average 0.11 radians of link rotation. When compared with the experimentally observed behavior it can be concluded that five of the frames considered in this study show satisfactory behavior and fracture of links is not expected under Maximum Considered Earthquake (MCE). The maximum demand for the 3 story frame with a bay width of 6 meters is 0.16 radians and it can potentially cause fracture of the bottom story link.

Future research should consider other factors that are not accounted for in this preliminary study. Different link length to bay width ratios requires further attention. In addition, the present study evaluated frames under the Maximum Considered Earthquake (MCE); however, the Methodology requires satisfactory behavior under seismic demands in excess of MCE. Only one failure criterion based on maximum link rotation angle was used for assessment purposes and future research should consider the cumulative link rotation angle demands. Performance of links with different types of stiffening also requires further attention. In general, the rotation capacity of the links is dependent on the stiffener spacing. Design link rotation angles and the calculated link rotation angles should be compared to make sure that these do not deviate significantly from each other resulting in lower link rotation angle capacities due to improper stiffening.

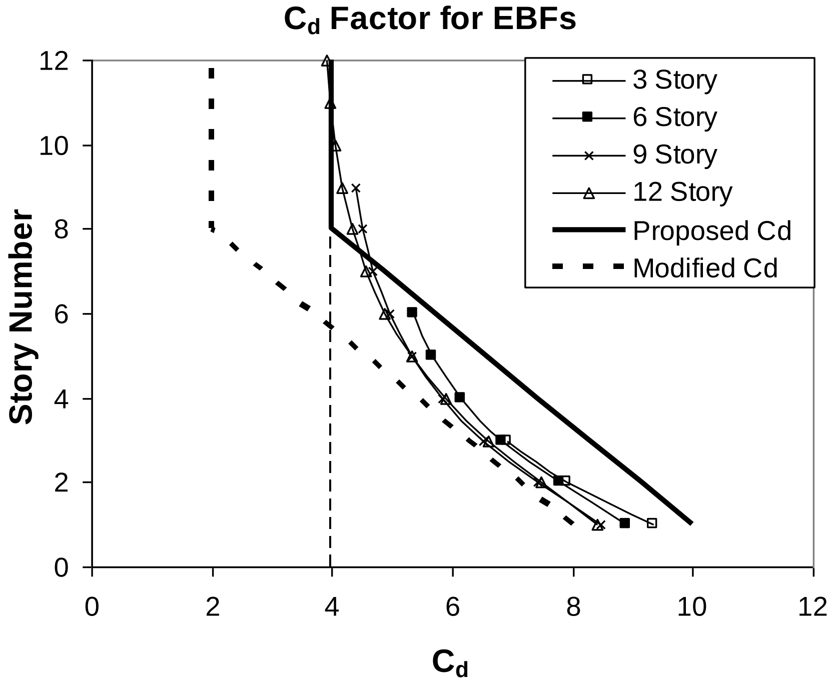

Fig. 10 Variation of C_d along the height

Story	Link	Brace	Column	Link	Brace	Column
	SDC D_{max} L=6m ns=3			SDC D_{max} L=10m ns=3		
1	W18×50	W8×58	W14×74	W18×40	W18×86	W14×68
2	W18×46	W8×58	W14×74	W14×38	W14×68	W14×68
3	W18×35	W8×48	W14×74	W8×40	W8×58	W14×68
	SDC D_{max} L=6m ns=6			SDC D_{max} L=10m ns=6		
1	W24×62	W14×74	W14×193	W18×50	W18×86	W14×132
2	W24×62	W14×74	W14×193	W18×50	W18×86	W14×132
3	W24×62	W14×74	W14×193	W18×40	W18×86	W14×132
4	W21×50	W8×67	W14×132	W12×35	W14×68	W14×53
5	W21×50	W8×67	W14×132	W8×40	W8×58	W14×53
6	W21×44	W8×67	W14×132	W8×40	W8×58	W14×53
	SDC D_{max} L=6m ns=9			SDC D_{max} L=10m ns=9		
1	W21×93	W18×86	W14×342	W21×57	W12×96	W14×233
2	W21×93	W18×86	W14×342	W21×57	W12×96	W14×233
3	W21×93	W18×86	W14×342	W18×55	W12×96	W14×233
4	W21×93	W18×86	W14×211	W18×46	W10×88	W14×145
5	W24×84	W10×77	W14×211	W18×46	W10×88	W14×145
6	W24×62	W14×74	W14×211	W18×46	W10×88	W14×145
7	W24×55	W10×68	W14×132	W18×46	W10×88	W14×74
8	W24×55	W10×68	W14×132	W16×45	W10×77	W14×74
9	W24×55	W10×68	W14×132	W16×45	W10×77	W14×74

Table 2 Member sizes of redesigned archetypes

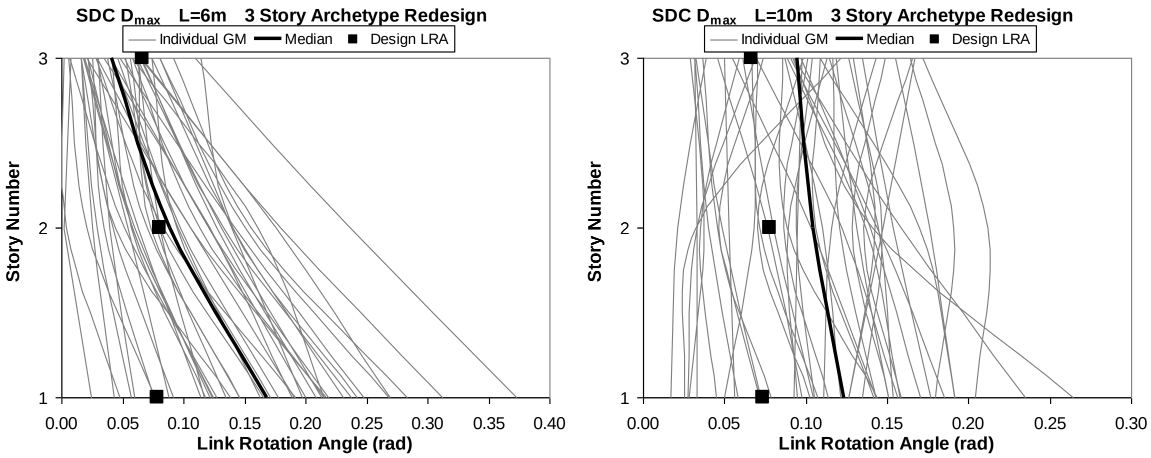

Fig. 11 Variation of link rotation angle for 3 story redesigned EBFs (SDC D_{max})

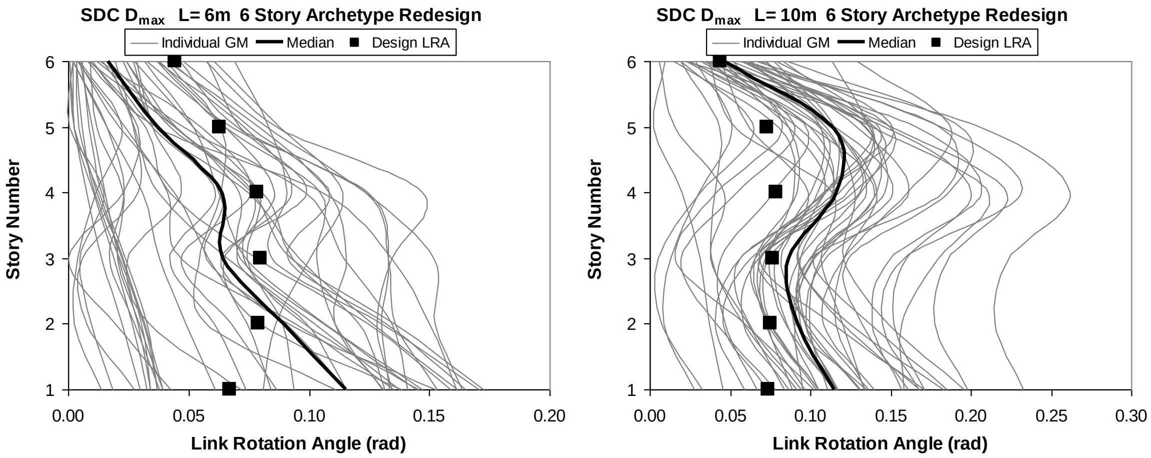

Fig. 12 Variation of link rotation angle for 6 story redesigned EBFs (SDC D_{max})

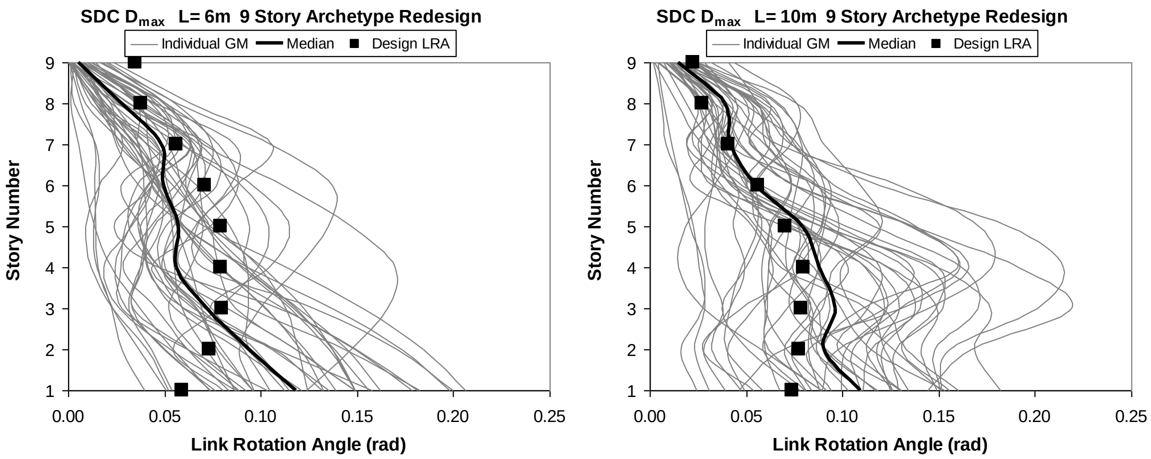

Fig. 13 Variation of link rotation angle for 9 story redesigned EBFs (SDC D_{max})

CONCLUSIONS

A numerical study on seismic performance factors of EBFs has been presented. The Methodology outlined in FEMA P695 was applied to EBFs to evaluate the response factors. Nonlinear time history analyses were conducted for 12 archetypes and the structures were subjected to the Maximum Considered Earthquake (MCE) ground motions. The results indicate that the link rotation angle demands at lower stories can be higher than typical rotation capacities. Higher values of demand were found to be related with the underestimations of lateral displacements and link rotation angles at the design stage. Modification to the deflection amplification factor was proposed and six of the problematic archetypes were redesigned based on the proposed modification. Analyses of redesigned archetypes reveal that the proposed modifications are adequate to reduce link rotation angle demands to acceptable levels.

REFERENCES

[1] POPOV EGOR, ENGELHARDT MICHAEL "Seismic eccentrically braced frames", *Journal of Constructional Steel Research*, Vol. 10, 1988, pp. 321-354.

[2] AMERICAN INSTITUTE OF STEEL CONSTRUCTION (AISC) "Seismic Provisions for Structural Steel Buildings ANSI/AISC 341-05", *American Institute of Steel Construction*, 2005, Chicago, IL.

[3] UANG CHIA-MING (1991) "Establishing R (or Rw) and Cd factors for building seismic provisions", *ASCE Journal of Structural Engineering,* Vol. 117, No.1, 1991, pp. 19-28.

[4] AMERICAN SOCIETY OF CIVIL ENGINEERS AND STRUCTURAL ENGINEERING INSTITUTE (ASCE/SEI) "Minimum Design Loads for Buildings and Other Structures", *American Society of Civil Engineers*, 2010, Reston, VA

[5] EUROCODE 8 "Design of structures for earthquake resistance – Part 1: General Rules, seismic actions and rules for buildings", *European Committee for Standardization*, 2004, Brussels, Belgium.

[6] CLIFTON CHARLES, BRUNEAU MICHEL, MACRAE GREG, LEON ROBERTO and FUSSELL ALISTAIR "Steel structures damage from the Christchurch Earthquake Series of 2010 and 2011", *Bulletin of The New Zealand Society for Earthquake Engineering*, Vol. 44, No. 4, 2011, pp. 297-318.

[7] FEDERAL EMERGENCY MANAGEMENT AGENCY (FEMA) "Quantification of Building Seismic Performance Factors FEMA P695 ATC-63 Project Report", *Federal Emergency Management Agency*, 2009, Washington, DC.

[8] OKAZAKI TAICHIRO, ENGELHARDT MICHAEL, NAKASHIMA MASAYOSHI and SUITA KEIICHIRO "Experimental performance of link-to-column connections in eccentrically braced frames", *Journal of Structural Engineering*, Vol. 132, No. 8, 2006, pp. 1201-1211.

[9] AMERICAN INSTITUTE OF STEEL CONSTRUCTION (AISC) "Seismic Provisions for Structural Steel Buildings ANSI/AISC 341-10", *American Institute of Steel Construction*, 2010, Chicago, IL.

[10] RICHARDS PAUL, UANG CHIA-MING "Effect of flange width-thickness ratio on eccentrically braced frames link cyclic rotation capacity", *Journal of Structural Engineering*, Vol. 131, No. 10, 2005, pp. 1546-1552.

[11] AMERICAN INSTITUTE OF STEEL CONSTRUCTION (AISC) "Specification for Structural Steel Buildings ANSI/AISC 360-05", *American Institute of Steel Construction*, 2005, Chicago, IL.
[12] KUŞYILMAZ AHMET, TOPKAYA CEM "Design overstrength of steel eccentrically braced frames", *International Journal of Steel Structures*, Vol. 13, No. 3, 2013, pp. 529-545.
[13] FILIPPOU FILIP "Finite Elements in Design, Evaluation and Analysis of Structures (FEDEASLAB)", *University of California, Berkeley*, 2001, California, CA.
[14] SARITAS AFSIN, FILIPPOU FILIP "Frame element for metallic shear-yielding members under cyclic loading", *Journal of Structural Engineering*, Vol. 135, No. 9, 2009, pp. 1115-1123.
[15] KUŞYILMAZ AHMET "Numerical studies on eccentrically braced frames", Ph.D. Thesis, *Middle East Technical University (METU)*, 2014, Ankara, Turkey.
[16] MALLEY JAMES, POPOV EGOR "Shear links in eccentrically braced Frames", *Journal of Structural Engineering*, Vol. 110, No. 9, 1984, pp. 2275-2295.
[17] OKAZAKI TAICHIRO, ARCE GABRIELA, RYU HAN-CHOUL and ENGELHARDT MICHAEL, "Experimental study of local buckling, overstrength, and fracture of links in eccentrically braced frames", *Journal of Structural Engineering*, Vol. 131, No.10, 2005, pp. 15–35.